

Spin-dependent magnetic focusing

Yuli Lyanda-Geller, L. P. Rokhinson and Stefano Chesi

Abstract. Gabriele Giuliani was fascinated by spin-dependent phenomena. Here we review experiments on spin separation in cyclotron motion, semiclassical theory of effects of spin-orbit interactions on cyclotron resonance, and theory of spin filtering by a quantum point contact in two-dimensional hole systems.

1. Introduction

It is a great honor to contribute to Gabriele Giuliani's memorial volume, and it has been a remarkable experience to work with Gabriele. In the past 15 years, Condensed Matter physicists became greatly interested in spin-dependent phenomena, creating a direction of research named 'spintronics' [1]. Gabriele was genuinely interested in this trend, involved his students in research in this field, and was instrumental in attracting several faculty members with interest in spin-dependent phenomena to the Purdue University Physics Department.

Among several interesting new phenomena discovered over the last decade, there is spin-dependent magnetic focusing [2–4]. Classical electron focusing was first observed in metals [5, 6]. Coherent electron focusing is most remarkably pronounced in semiconductor nanostructures, where it became a signature phenomenon for quantum ballistic transport [7]. When two quantum point contacts in a two-dimensional electron gas are separated by multiples of the cyclotron diameter, injection from one point contact results in an additional potential developed across the detector point contact. It has been long appreciated that signature quantum effects, such as the Aharonov-Bohm effect, have remarkable spin counterparts due to spin-orbit interactions [8, 9]. In [2], it has been discovered that the effect of magnetic focusing can be used as spin filter.

This work was supported by the U.S. Department of Energy, Office of Basic Energy Sciences, Division of Materials Sciences and Engineering under Award DE-SC0010544 (Y.L-G), and by the National Science Foundation under Grant No. 1307247-DMR (L.P.R.).

The origin of such filtering can be traced to spin-orbit interactions introducing a dependence of the cyclotron radius on the spin of the charge carriers.

Gabriele Giuliani recognized that several features observed in magnetic focusing experiments in two-dimensional hole gases are unaccounted for in a semiclassical theory of magnetic focusing. More specifically, Gabriele was intrigued by the reappearance of a filtered spin component at high in-plane magnetic fields. That led to the paper where a theory of spin-dependent transmission through quantum point contacts in the two-dimensional hole gas (2DHG) has been developed [10]. In the present paper, which is our tribute to Gabriele, we review the results of experiments on spin-dependent focusing, discuss the semiclassical theory of spin-dependent focusing, and the spin filtering by quantum point contacts in the presence of spin-orbit interactions.

2. Experiment

To demonstrate spatial separation of spins experimentally we fabricated several 2DHG devices in the magnetic focusing geometry, see the inset in Figure 1. The structure is formed using atomic force microscopy local anodic oxidation technique (AFM LAO) [11–13]. Oxide lines separate the 2DHG underneath by forming ~ 200 mV potential barriers. A specially designed heterostructure is grown by MBE on [113]A GaAs. Despite very close proximity to the surface (350\AA), the 2DHG has an exceptionally high mobility $0.4 \cdot 10^6$ V·s/cm² and relatively low hole density $n = 1.38 \cdot 10^{11}$ cm⁻². The device consists of two QPCs oriented along the $[3\bar{3}2]$ crystallographic direction, separated by a central gate; the lithographically defined distance between QPCs is $L = 0.8$ μm . Potential in the point contacts is controlled separately by two gates G_{inj} and G_{det} , or by the central gate G_C . In our experiments the central gate was kept at -0.3 V and ~ 0.2 V were applied to the gates G_{inj} and G_{det} . Asymmetric biasing of point contacts provides sharper confining potential and reduces the distance between the two potential minima by $\Delta L \sim 0.07$ μm .

Magnetic focusing manifests itself as equidistant peaks in the magnetoresistance $R(B_\perp)$ for only one direction of B_\perp . R is measured by applying a small current through the injector QPC while monitoring voltage across the detector QPC. At $B_\perp < 0$, cyclotron motion forces the carriers away from the detector. Then, only the 2DHG contributes to R , which has almost no B_\perp -dependence at low fields and shows Shubnikov–de Haas oscillations at $|B_\perp| > 0.3$ T. For $B_\perp > 0$, several peaks due to magnetic focusing are observed. The peak separation $\Delta B \approx 0.18$ T is consistent with the distance between the injector and detector QPCs. The data is

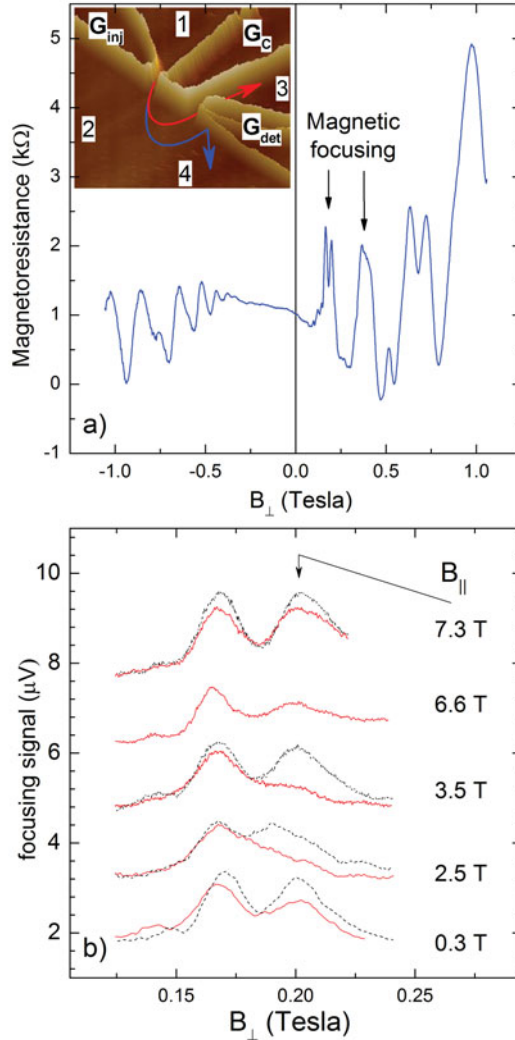


Figure 1. a) Magnetoresistance and layout of focusing devices. The voltage across the detector (contacts 3 and 4) is measured as a function of magnetic field perpendicular to the surface of the sample (B_{\perp}). The lithographical separation between point contacts is $0.8 \mu\text{m}$. A current of 1 nA is flowing through the injector (contacts 1 and 2). The positions of the magnetic focusing peaks are marked with arrows. Inset: AFM micrograph of a sample ($5\mu\text{m} \times 5\mu\text{m}$). Light lines are the oxide which separates different regions of the 2D hole gas. The semicircles show schematically the trajectories for two spin orientations. b) Focusing signal for the first focusing peak in a tilted magnetic field, plotted versus B_{\perp} . The values of the corresponding B_{\parallel} , for $B_{\perp} = 0.2$ T, are marked on the right. Curves are offset for clarity. The dashed black (solid red) curves correspond to $G_{inj} = 2e^2/h$ ($< e^2/h$).

symmetric upon exchange of the injector and detector and simultaneous reversal of the magnetic field direction.

When the conductance of both QPCs is tuned to be $2e^2/h$, the first focusing peak splits into two peaks. When the in-plane component is $B_{\parallel} = 0$ the peaks in the doublet have approximately the same height. If the conductance of the injector QPC is $G_{inj} < 2e^2/h$ the rightmost peak is slightly suppressed, which has been interpreted as due to spontaneous polarization [14].

We use the spin filtering by QPCs in the presence of in-plane magnetic field B_{\parallel} to probe the spin states which correspond to the first focusing peak doublet. Applying B_{\parallel} along $[3\bar{3}\bar{2}]$ affects the energies of the spin subbands without affecting the cyclotron motion. As the Zeeman splitting of the spin subbands in a 2D gas increases, preferential transmission of the largest- k_F spin subband is expected for electrons, corresponding to suppression of the *left* peak. Instead, in a hole gas we observe suppression of the *right* peak up to $B_{\parallel} \approx 2.5$ T, see Figure 1 b. For $B_{\parallel} > 2.5$ T the right peak reappears and at $B_{\parallel} = 7.3$ T becomes as prominent as the left one.

3. Theory

There has been a considerable interest to understand hole spectra in low dimensional systems over the past decade, also in connection with research in the field of quantum computing. Of special interest are heterostructures grown along the $[001]$ direction, in which the hole spectra are remarkably different from electron spectra. In this case, several authors concluded that intrinsic Dresselhaus and Rashba spin-orbit interactions are cubic in the wavevector [17], and that the in-plane g -factor describing the Zeeman splitting of holes with an in-plane magnetic field is quadratic in electron momentum and depends on its orientation. As it turns out, however, earlier work [19] pointed out that for this crystallographic orientation of the 2DHG, the Dresselhaus term gives rise to contributions linear in momentum. Furthermore, approaches based on low-order perturbation theory are generally oversimplified because, as was discussed in [20], do not take properly into account the non-perturbative effect of a mutual transformation of heavy and light holes upon reflection from the walls of the quantum well [21–23]. This effect results in the presence of two standing hole waves in the wavefunctions of hole states, corresponding to heavy and light holes moving along the growth direction, as opposed to electron case with only one standing wave. Taking mutual transformation of heavy and light holes into account considerably alters the in-plane effective mass of holes, and the coupling constants of

the intrinsic spin-orbit interaction as well. Numerical simulations taking into account a finite number of levels of spatial quantization in the [001] growth direction might also lead to inaccurate results, if proper care is not taken upon truncation of the Hilbert space, because all levels of size quantization result in contributions to the in-plane effective mass and cubic spin-orbit splitting characterized by the same physical scale (*i.e.*, all contributions have in principle the same order of magnitude).

Our knowledge of properties of holes in quantum wells grown along the [113] crystallographic orientation is even less extensive. Existing analytical results [15, 16] were obtained in the so-called axial approximation [17], which may take into account effects of the mutual transformation of heavy and light holes upon reflection from the walls of the quantum well only partially. Numerical work was performed which should give more accurate results [10]. Although a progressively larger number of spatial quantization levels were included, until the numerical spectra did not change significantly, a more careful analysis of truncation errors seems necessary in the light of the non-perturbative nature of the effects described above [20–23]. Nevertheless, conclusions about certain properties can be drawn on symmetry grounds from the properties of [001]-grown structures. In particular, quantization along the [113] crystallographic direction mixes in-plane and out-of-plane properties of the [001] structures, which results in a contribution to the in-plane g -factor independent of wavevector. This contribution is non-zero only because the bulk spectrum of holes is anisotropic. Both cubic- and linear-in-momentum Rashba and Dresselhaus spin-orbit interactions are present in the [113] configuration, and the linear in momentum Rashba spin-orbit term is related to the anisotropy of the bulk hole spectra. Although the precise magnitude and angular dependence of these interactions is not known, we will describe how simple models explain the experimental data on focusing in [113]-oriented hole quantum wells.

4. Semiclassical theory of focusing

It has long been appreciated that intrinsic spin-orbit (SO) interactions can be interpreted as an effective momentum-dependent magnetic field that influences the spin of charge carriers [24]. More recently, it has been recognized [8, 9, 25–27] that SO interactions can be also viewed as an effective orbital magnetic field with an opposite sign for different spin orientations. In order to explain the effect of spin filtering in magnetic focusing qualitatively, it is reasonable to assume that charge carriers in GaAs quantum well are characterized by an isotropic kinetic energy and the Dresselhaus intrinsic spin-orbit interaction linear in the hole momentum.

Indeed, for the lowest hole states in a 2DHG in both [113] and [001] configurations, a linear Dresselhaus term is present. The simplified hole Hamiltonian can be written as $H = \frac{1}{2m}(p_x + \beta\sigma_x)^2 + \frac{1}{2m}(p_y - \beta\sigma_y)^2$, where m is the effective mass, \vec{p} is the electron momentum, σ_i are the Pauli matrices ($i = x, y$), and β is the SO parameter. For simplicity it is also reasonable to neglect anisotropy of the effective mass as this assumption does not change the qualitative picture. In the semiclassical description, appropriate for the range of magnetic fields B_\perp used for the focusing experiments, the motion is described by simple equations:

$$\begin{aligned} \frac{d\vec{p}}{dt} &= e\vec{v} \times \vec{B} & \vec{v} &= \frac{d\vec{r}}{dt} = \frac{\partial \epsilon_\pm(\vec{p})}{\partial \vec{p}} \\ \epsilon_\pm &= \frac{1}{2m}(p \pm \beta)^2 + \frac{\beta^2}{2m}, \end{aligned} \quad (4.1)$$

where \vec{r} , \vec{v} and ϵ_\pm are the charge carrier coordinate, velocity and energy for the two spin projections. This description implies that the carrier wavelength is smaller than the cyclotron radius, and that jumps between orbits with different spin projections are absent, *i.e.*, $\epsilon_f \gg \beta p/m \gg \hbar\omega_c$. Equation (4.1) show that the charge carrier with energy $\epsilon_\pm = \epsilon_f$ is characterized by a spin-dependent trajectory with momentum \vec{p}_\pm , coordinate \vec{r}_\pm , and cyclotron frequency ω_c^\pm . The solution to these equations is

$$\begin{aligned} p_\pm^{(x)} + ip_\pm^{(y)} &= p_\pm \exp(-i\omega_c^\pm t) \\ r_\pm^{(x)} + ir_\pm^{(y)} &= \frac{i\sqrt{2m\epsilon_f}}{m\omega_c^\pm} \exp(-i\omega_c^\pm t) \\ \omega_c^\pm &= \frac{eB_\perp}{m}(1 \pm \beta/p_\pm). \end{aligned} \quad (4.2)$$

Thus, the cyclotron motion is characterized by a spin-dependent field $B_\pm = B_\perp(1 \pm \beta/p_\pm) = B_\perp \pm B_{so}$, where B_{so} is the SO effective field characterizing the cyclotron motion. Using a semiclassical limit of the quantum description [28], one obtains identical results.

In the focusing configuration, QPCs are used as monochromatic point sources. Holes, injected in the direction perpendicular to the 2DHG boundary, can reach the detector directly or after specular reflections from the boundary. As follows from Eqs. (4.2), for each of the two spin projections there is a characteristic magnetic field such that the point contact separation is twice the cyclotron radius for a given spin, $L = 2R_\pm^c = 2p_f/eB_\pm$, $p_f = \sqrt{2m\epsilon_f}$. The first focusing peak occurs at

$$B_\perp^\pm = \frac{2(p_f \mp \beta)}{eL}. \quad (4.3)$$

The magnitude of β can be calculated directly from the peak splitting $\beta = (B_{\perp}^{+} - B_{\perp}^{-})eL/4 = 7 \cdot 10^{-9} \text{ eV}\cdot\text{s/m}$. A larger value of $\beta \approx 25 \cdot 10^{-9} \text{ eV}\cdot\text{s/m}$ was extracted from the splitting of the cyclotron resonance at 3 times higher hole concentration [29]. We note that Equation (4.3) is more general than the Eqs. (4.2). The coefficient β essentially describes the separation in momentum space of the two parts of the Fermi surface which correspond to $\epsilon^{\pm} = \epsilon_f$, and includes contributions of various spin-orbit terms in the 2DHG.

The difference of the spin-dependent focusing field B_{\perp}^{\pm} is proportional to β and does not depend on the cyclotron frequency $\omega_c = eB_{\perp}/m$. At the same time, the difference of spin-dependent cyclotron frequencies in Equation (4.2) is proportional to both ω_c and β . Thus, the effective magnetic field B_{so} is itself proportional to B_{\perp} . This effect differs from the spin-dependent shift of the Aharonov-Bohm oscillations in the conductance of rings, where the additional spin-orbit flux and the Aharonov-Bohm flux are independent of each other [9]. If the Zeeman effect is taken into account, both ω_c^{\pm} and R_c^{\pm} acquire an additional dependence on B_{\perp} , as well as on the in-plane component B_{\parallel} .

5. Focusing peaks in in-plane magnetic field

The behavior of the focusing peaks in Figure 1b requires to consider simultaneously the charge carriers motion in the 2DHG and their transmission through quantum point contacts. The observed results cannot be explained by considering only an intrinsic spin-orbit coupling of the 2D hole system linear-in-momentum. Furthermore, both 2D Dresselhaus and Rashba SO terms which are cubic-in-momentum necessarily generate additional linear-in-momentum contributions within the quantum point contact, similar to the generation of both cubic and linear terms in the 2D electron Hamiltonian from the bulk cubic Dresselhaus terms. To illustrate the physics of filtering by point contacts we consider, for example, an Hamiltonian with the cubic Rashba term of the form $\frac{i\gamma}{2} (\hat{p}_-^3 \hat{\sigma}_+ - \hat{p}_+^3 \hat{\sigma}_-)$. Here, $\hat{p}_{\pm} = \hat{p}_x \pm i\hat{p}_y$ and $\hat{\sigma}_{\pm} = \hat{\sigma}_x \pm i\hat{\sigma}_y$. Such cubic spin-orbit interaction is responsible for a peculiar dispersion of the lowest two one-dimensional (1D) subbands. For a channel with lateral extent W , aligned with the x -axis, we can substitute $\langle p_y^2 \rangle \sim (\hbar\pi/W)^2$ and $\langle p_y \rangle \sim 0$ in the 2D Hamiltonian, which gives

$$\hat{H}_{1D} = \frac{\hat{p}_x^2}{2m} + \gamma \left(\frac{3\hbar^2\pi^2}{W^2} \hat{p}_x - \hat{p}_x^3 \right) \hat{\sigma}_y + \frac{\hbar^2\pi^2}{2mW^2}. \quad (5.1)$$

Due to the lateral confinement, a linear spin-orbit term appears in Equation (5.1), which is dominant at small momenta and coexist with a cubic

contribution with opposite sign. Therefore, spin subbands in such a case cross not only at $k_x = 0$, but also at finite wave vectors $k_x = \pm \frac{\sqrt{3}\pi}{W}$. In [10], the spin splitting due to Rashba term in quantum point contacts was computed numerically taking into account up to 10 levels of size quantization in the quantum well for various applied electric fields, as shown in Figure 2. The 1D bands clearly display the main feature: the presence of a crossing point at finite wave vector.

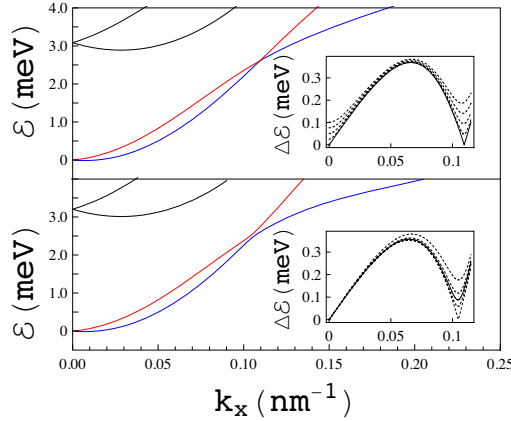


Figure 2. Energy subbands of 1D channels obtained from a 15 nm quantum well grown in the [113] direction. An electric field $\mathcal{E}_z = 1 \text{ V}/\mu\text{m}$ along [113] is present. The lateral confinement has width $W = 40 \text{ nm}$. Upper panel: wire along $[3\bar{3}2]$. The inset shows the energy splitting of the two lowest subbands at several values of B_{\parallel} . The solid curve is for $B_{\parallel} = 0$ and the dashed curves for $B_{\parallel} = 0.5, 1, \dots, 2.5 \text{ T}$. Lower panel: wire along $[1\bar{1}0]$. The inset shows the energy splitting with a lateral electric field. The solid curve is for $\mathcal{E}_y = 0$ and the dashed curves for $\mathcal{E}_y = \pm 0.05, \pm 0.015 \text{ V}/\mu\text{m}$ (the splitting is reduced for negative values of \mathcal{E}_y).

As illustrated by the inset of Figure 2 (first panel), the degeneracies at $k_x = 0$ and finite k_x are removed when $B_{\parallel} \neq 0$. Within the effective Hamiltonian (5.1), an external magnetic field is taken into account by adding a Zeeman term $g^* \mu_B B_{\parallel} \hat{\sigma}_x / 2$, where g^* is the effective g -factor [30] and μ_B the Bohr magneton. The total effective magnetic field, which includes spin-orbit interactions, depends on values of W and k_x as follows

$$\vec{B}_{eff}(W, k_x) = B_{\parallel} \hat{x} + \frac{2\gamma \hbar^3}{g^* \mu_B} \left(\frac{3\pi^2}{W^2} k_x - k_x^3 \right) \hat{y}, \quad (5.2)$$

where \hat{x}, \hat{y} are unit vectors along the coordinate axes. The eigenstates of Equation (5.1), $\psi_W(k_x, \pm) = e^{ik_x x} |k_x, \pm\rangle_W$, have spinor functions

$|k_x, \pm\rangle_W$ parallel/antiparallel to \vec{B}_{eff} and energies

$$\epsilon_{\pm}(W, k_x) = \frac{\hbar^2 k_x^2}{2m} \mp \frac{1}{2} g^* \mu_B |\vec{B}_{eff}(W, k_x)|. \quad (5.3)$$

At $k_x = 0$ and $k_x = \pm\sqrt{3}\pi/W$ the spin splitting is $g^* \mu_B B_{\parallel}$, *i.e.*, it is only due to the external magnetic field.

In a realistic QPC the width $W(x)$ of the lateral confinement changes along the channel. As in [31], a sufficiently smooth variation of the width is assumed, such that holes adiabatically follow the lowest *orbital* subband. Introducing in Equation (5.1) a x -dependent width $W(x) = W_0 e^{x^2/2\Delta x^2}$, where Δx is a typical length scale of the QPC and W_0 its minimum width, one obtains the following effective Hamiltonian

$$\begin{aligned} \hat{H}_{QPC} = & \frac{\hat{p}_x^2}{2m} + V(\hat{x}) + \frac{g^* \mu_B}{2} B_{\parallel} \hat{\sigma}_x \\ & + \gamma [3m\{V(\hat{x}), \hat{p}_x\} - \hat{p}_x^3] \hat{\sigma}_y, \end{aligned} \quad (5.4)$$

with $\{a, b\} = ab + ba$ [32]. The potential barrier has the following form:

$$V(x) = \frac{\hbar^2 \pi^2}{2m W(x)^2} = \frac{\hbar^2 \pi^2}{2m W_0^2} e^{-x^2/\Delta x^2}. \quad (5.5)$$

The main qualitative conclusions are independent of the detailed form of the potential, but Equation (5.5) allows to solve explicitly the 1D transmission problem and obtain a spin-resolved conductance in the Landauer-Büttiker formalism. The scattering eigenstates are obtained with incident wavefunctions $\psi_{W=\infty}(k_{\mu}, \mu)$ at $x \ll -\Delta x$, where $\mu = \pm$ denotes the spin subband and k_{\pm} are determined by the Fermi energy ϵ_f , at which the holes are injected in the QPC. For $x \gg \Delta x$, such QPC wavefunctions have the asymptotic form $\sum_{v=\pm} t_{\mu,v} \psi_{\infty}(k_v, v)$, where $t_{\mu,v}$ are transmission amplitudes. The spin-resolved conductances are simply given by $G_{\pm} = \frac{e^2}{h} \sum_{\mu=\pm} \frac{v_{\pm}}{v_{\mu}} |t_{\mu,\pm}|^2$ [33], where the Fermi velocities are $v_{\pm} = \frac{\partial \epsilon_{\pm}(\infty, k_{\pm})}{\partial \hbar k_x}$, from Equation (5.3). The total conductance is $G = G_+ + G_-$. Typical results at several values of B_{\parallel} are shown in Figure 3. As usual, by opening the QPC, a current starts to flow above a minimum value of W_0 and, with a finite magnetic field, $G_+ \neq G_-$. At zero magnetic field, there is structureless unpolarized conductance ($G_+ = G_-$). At larger magnetic fields, $G_- > G_+$, *i.e.*, holes in the *higher* spin subband have larger transmission at the first plateau. The sign is opposite to the case of linear Rashba spin-orbit coupling (see [34]) and in agreement with the experimental results of Figure 1. For a magnetic field $B_{\parallel} \approx 7$ T (see

the third panel of Figure 3) $G_+ \simeq G_-$ and the transmission becomes unpolarized, as observed in the data of Figure 1. Finally, at even larger values of $B_{\parallel} > 7$ T, $G_+ \simeq e^2/h$, $G_- \simeq 0$ (fourth panel of Figure 3). For such sufficiently large magnetic field the role of the spin-orbit coupling becomes negligible and the spin direction (parallel/antiparallel to the external magnetic field) of the holes is conserved. The injected holes remain in the original (+ or -) branch and the current at the first plateau is polarized in the + band, which has lower energy. Deviations from this behavior are due to non-adiabatic transmission in the spin subband. In order to gain a qualitative understanding, we consider the semiclassical picture of the hole motion in quantum point contact.

When a hole wave-packet is at position x , it is subject to a magnetic field \vec{B}_{eff} determined by $W(x)$ and $k_x(x)$ as in Equation (5.2). For holes injected at ϵ_f , the momentum is determined by energy conservation. Treating the spin-orbit coupling as a small perturbation compared to the kinetic energy, one has $k_x(x) \simeq \sqrt{k_f^2 - \pi^2/W(x)^2}$, where $k_f = \sqrt{2m\epsilon_f}/\hbar$ is the Fermi wave-vector in the absence of spin-orbit coupling. Therefore, the injected hole experiences a varying magnetic field in its semiclassical motion along x , due to the change of both k_x and $W(x)$. For adiabatic transmission of the spin subbands, the spin follows the direction of the magnetic field, but this is not possible in general if B_{\parallel} is sufficiently small. In particular, for $B_{\parallel} = 0$ Equation (5.1) implies that $\hat{\sigma}_y$ is conserved. Therefore, the initial spin orientation along y is not affected by the motion of the hole. On the other hand, \vec{B}_{eff} of Equation (5.2) changes direction when $k_x = \sqrt{3}\pi/W$. After this point, a hole in the + branch continues its motion in the - branch and vice-versa.

At finite in-plane magnetic field the degeneracy of the spectrum is removed but the holes do not follow adiabatically the spin branch, unless the Landau-Zener condition $\frac{dB_y/dt}{B_{\parallel}} \ll \omega_B$ is satisfied, where $\hbar\omega_B = g^*\mu_B B_{\parallel}$. The change ΔB_y in the spin-orbit field is obtained from Equation (5.2): $|B_y|$ is equal to $2\gamma\hbar^3 k_f^3/g^*\mu_B$ far from the QPC and vanishes at the degeneracy point. This change occurs on the length scale Δx of the QPC, and the estimate of the time interval is $\Delta t \simeq \Delta x/v$, where v is a typical velocity of the hole. This gives

$$B_{\parallel} \gg \sqrt{\frac{\hbar\Delta B_y}{g^*\mu_B\Delta t}} \simeq \frac{\hbar^2\sqrt{2\gamma k_f^3 v/\Delta x}}{g^*\mu_B}. \quad (5.6)$$

The estimate of v at the degeneracy point $k_x = \sqrt{3}\pi/W$ is obtained from $\sqrt{3}\pi/W \simeq \sqrt{k_f^2 - \pi^2/W^2}$, which gives $k_x = \frac{\sqrt{3}}{2}k_f$. Therefore, v is

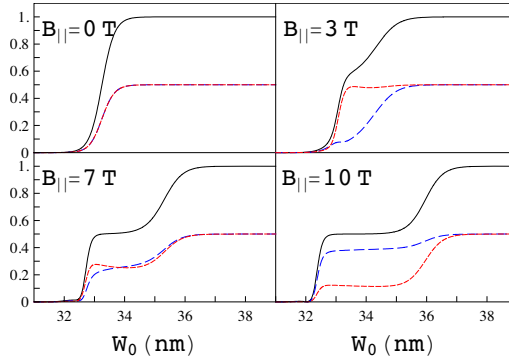


Figure 3. Total conductance G (black solid curves) and spin-resolved conductances G_+ (blue, long-dashed) and G_- (red, short-dashed), plotted in units of $2e^2/h$ as functions of the minimum width W_0 of the QPC [see Equation (5.5)]. In these simulations, $m = 0.14m_0$ [16], where m_0 is the bare electron mass, $g^* = 0.8$ [30], $\gamma\hbar^3 = 0.45 \text{ eV nm}^3$, $\Delta x = 0.3\mu\text{m}$, and $\epsilon_f = 2.3 \text{ meV}$.

large at the degeneracy point ($v \simeq v_f$, where $v_f = \hbar k_f/m$ is the Fermi velocity), and to follow adiabatically the spin branches requires a large external field. The crossover occurs for

$$B^* \simeq \frac{(\hbar k_f)^2 \sqrt{2\gamma\hbar/(m\Delta x)}}{g^* \mu_B}. \quad (5.7)$$

Below B^* , holes injected in the $+$ band cross non-adiabatically to the $-$ spin branch when $k_x \simeq \sqrt{3}\pi/W$. Therefore, holes injected in the lower subband have higher energy at $x \simeq 0$ and are preferentially reflected, as seen in the second panel of Figure 3 (with $B_{\parallel} = 3 \text{ T}$). The reflection is not perfect, due to non-adiabaticity at $k_x \simeq 0$: at this second quasi-degenerate point the $-$ holes can cross back to the $+$ branch, and be transmitted.

This discussion shows that, in a model where the cubic Rashba term of 2D holes gives rise to both linear- and cubic-in-momentum terms in the QPC, the degeneracy of the hole spectrum at $k_x = \sqrt{3}\pi/W$ is crucial to obtain the anomalous transmission of Figures 1 and 3. We expect that when all cubic and linear terms are taken into account, arising from both Rashba and Dresselhaus SO interactions, the result will be qualitatively the same.

6. Conclusion

The cyclotron motion makes it possible to spatially separate spin currents in materials with sufficiently strong intrinsic spin-orbit interactions.

We have understood the physical mechanisms which give rise to spin-dependent magnetic focusing and the anomalous spin filtering by quantum point contacts. Professor Gabriele Giuliani made important contributions to the theory and our current understanding of spin-dependent magnetic focusing, as well as in the broader field of spintronics and spin transport.

References

- [1] D. D. AWSCHALOM, D. LOSS and N. SAMARTH (eds.), *Semiconductor Spintronics and Quantum Computation*, Springer, New York, 2002.
- [2] L. P. ROKHINSON, V. LARKINA, Y. B. LYANDA-GELLER, L. N. PFEIFFER and K. W. WEST, *Phys. Rev. Lett.* **93** (2004), 146601.
- [3] B.I. HALPERIN, Commentary, *Journal Club for Condensed Matter Physics*, July 2004.
- [4] *Directing Matter and Energy: Five Challenges for Science and Imagination*. A report from Department of Energy Basic Energy Sciences Advisory Committee (2007), p. 5.
- [5] Y. V. SHARVIN, *Zh. Eksp. Teor. Fiz.* **48** (1965), 984 [*Sov. Phys. JETP* **21** (1965), 655].
- [6] V. S. TSOI, *JETP Letters* **22** (1975), 197.
- [7] H. VANHOUTEN, C. W. J. BEENAKKER, J. G. WILLIAMSON, M. E. I. BROEKAART, P. H. M. VANLOOSDRECHT, B. J. VANWEES, J. E. MOOIJ, C. T. FOXON and J. J. HARRIS, *Phys. Rev. B* **39** (1989), 8556.
- [8] Y. AHARONOV and A. CASHER, *Phys. Rev. Lett.* **53** (1984), 319.
- [9] A. G. ARONOV and Y. B. LYANDA-GELLER, *Phys. Rev. Lett.* **70** (1993), 343.
- [10] S. CHESI, G. GIULIANI, L. P. ROKHINSON, L. PFEIFFER and K. WEST, *Phys. Rev. Lett.* **106** (2011), 236601.
- [11] E. S. SNOW and P. M. CAMPBELL, *Appl. Phys. Lett.* **64** (1994), 1932.
- [12] R. HELD, T. HEINZEL, A. P. STUDERUS, K. ENSSLIN and M. HOLLAND, *Appl. Phys. Lett.* **71** (1997), 2689.
- [13] L. P. ROKHINSON, D. C. TSUI, L. N. PFEIFFER and K. W. WEST, *Superlattices Microstruct.* **32** (2002), 99.
- [14] L. P. ROKHINSON, L. N. PFEIFFER and K. W. WEST, *Phys. Rev. Lett.* **96** (2006), 156602.
- [15] S. CHESI, unpublished
- [16] T. MINAGAWA, PhD Thesis, Purdue University, 2010,

- [17] R. WINKLER, “Spin-Orbit Coupling Effects in Two-Dimensional Electron and Hole Systems”, Springer, Berlin, 2003.
- [18] R. WINKLER, Phys. Rev. B **62** (2000), 4245; R. WINKLER, H. NOH, E. TUTUC and M. SHAYEGAN, Phys. Rev. B **65** (2002), 155303; S. CHESI and G. F. GIULIANI, Phys. Rev. B **75** (2007), 155305.
- [19] E. I. RASHBA and E. YA. SHERMAN, Phys. Lett. A **129** (1988), 175.
- [20] Y. LYANDA-GELLER, ArXiv:1210.7825
- [21] S. S. NEDOREZOV, Sov. Phys. Solid State **12** (1971), 1814 [Fizika Tverdogo Tela, 12, 2269 (1970)],
- [22] I. A. MERKULOV, V. I. PEREL’ and M. E. PORTNOI, Zh. Eksper. Teor. Fiz **99** (1991), 1202 [Sov Phys. JETP, **72** 660 (1991)].
- [23] M. I. DYAKONOV and A. V. KHAETSKII, Zh. Eksp. Teor Fiz. **82** (1982), 1584 [Sov. Phys. JETP, 55 917 (1982)].
- [24] E. I. RASHBA, Sov. Phys. Solid State **2** (1960), 1109.
- [25] D. LOSS, P. GOLDBART and A. V. BALATSKY, Phys. Rev. Lett. **65** (1990), 1655.
- [26] S. V. IORDANSKII, YU. B. LYANDA-GELLER and G. E. PIKUS, JETP Letters **60** (1994), 206.
- [27] I. L. ALEINER and V. I. FALKO, Phys. Rev. Lett. **87** (2001), 256801.
- [28] Y. A. BYCHKOV and E. I. RASHBA, JETP Lett. **39** (1984), 78.
- [29] H. L. STORMER, Z. SCHLESINGER, A. CHANG, D. C. TSUI, A. C. GOSSARD and W. WIEGMANN, Phys. Rev. Lett. **51** (1983), 126.
- [30] R. DANNEAU *et al.*, Phys. Rev. Lett. **97** (2006), 026403; S. P. KODUVAYUR *et al.*, Phys. Rev. Lett. **100** (2008), 126401.
- [31] L. I. GLAZMAN, G. B. LESOVIK, D. E. KHMEL’NITSKII and R. I. SHEKHTER, JETP Lett. **48** (1988), 238.
- [32] The anticommutator is introduced to obtain a hermitian Hamiltonian. This has negligible effect in the limit of a smooth contact, when $\partial V/\partial x$ is small.
- [33] G_{\pm} is defined for unpolarized incident holes and spin-resolved detection.
- [34] A. REYNOSO, G. USAJ and C. A. BALSEIRO, Phys. Rev. B **75** (2007), 085321.